IQGAP1 Is Important for Activation of Caspase-1 in Macrophages and Is Targeted by *Yersinia pestis* Type III Effector YopM

Lawton K. Chung,[a] Naomi H. Philip,[b] Valentina A. Schmidt,[c] Antonius Koller,[d] Till Strowig,[e] Richard A. Flavell,[e] Igor E. Brodsky,[b] James B. Bliska[a]

Department of Molecular Genetics and Microbiology and Center for Infectious Diseases, Stony Brook University, Stony Brook, New York, USA[a]; Department of Pathobiology, School of Veterinary Medicine, University of Pennsylvania, Philadelphia, Pennsylvania, USA[b]; Department of Medicine[c] and Proteomics Center,[d] School of Medicine, Stony Brook University, Stony Brook, New York, USA; Department of Immunobiology and Howard Hughes Medical Institute, Yale University School of Medicine, New Haven, Connecticut, USA[e]

ABSTRACT YopM is a leucine-rich repeat (LRR)-containing effector in several *Yersinia* species, including *Yersinia pestis* and *Y. pseudotuberculosis*. Different *Yersinia* strains encode distinct YopM isoforms with variable numbers of LRRs but conserved C-terminal tails. A 15-LRR isoform in *Y. pseudotuberculosis* YPIII was recently shown to bind and inhibit caspase-1 via a YLTD motif in LRR 10, and attenuation of YopM$^-$ YPIII was reversed in mice lacking caspase-1, indicating that caspase-1 inhibition is a major virulence function of YopM^{YPIII}. To determine if other YopM proteins inhibit caspase-1, we utilized *Y. pseudotuberculosis* strains natively expressing a 21-LRR isoform lacking the YLTD motif (YopM^{32777}) or ectopically expressing a *Y. pestis* 15-LRR version with a functional (YopM^{KIM}) or inactivated (YopM^{KIM} D$_{271}$A) YLTD motif. Results of mouse and macrophage infections with these strains showed that YopM^{32777}, YopM^{KIM}, and YopM^{KIM} D$_{271}$A inhibit caspase-1 activation, indicating that the YLTD motif is dispensable for this activity. Analysis of YopM^{KIM} deletion variants revealed that LRRs 6 to 15 and the C-terminal tail are required to inhibit caspase-1 activation. YopM^{32777}, YopM^{KIM}, and YopM^{KIM} deletion variants were purified, and binding partners in macrophage lysates were identified. Caspase-1 bound to YopM^{KIM} but not YopM^{32777}. Additionally, YopM^{KIM} bound IQGAP1 and the use of *Iqgap1$^{-/-}$* macrophages revealed that this scaffolding protein is important for caspase-1 activation upon infection with YopM$^-$ *Y. pseudotuberculosis*. Thus, while multiple YopM isoforms inhibit caspase-1 activation, their variable LRR domains bind different host proteins to perform this function and the LRRs of YopM^{KIM} target IQGAP1, a novel regulator of caspase-1, in macrophages.

IMPORTANCE Activation of caspase-1, mediated by macromolecular complexes termed inflammasomes, is important for innate immune defense against pathogens. Pathogens can, in turn, subvert caspase-1-dependent responses through the action of effector proteins. For example, the *Yersinia* effector YopM inhibits caspase-1 activation by arresting inflammasome formation. This caspase-1 inhibitory activity has been studied in a specific YopM isoform, and in this case, the protein was shown to act as a pseudosubstrate to bind and inhibit caspase-1. Different *Yersinia* strains encode distinct YopM isoforms, many of which lack the pseudosubstrate motif. We studied additional isoforms and found that these YopM proteins inhibit caspase-1 activation independently of a pseudosubstrate motif. We also identified IQGAP1 as a novel binding partner of the *Yersinia pestis* YopM^{KIM} isoform and demonstrated that IQGAP1 is important for caspase-1 activation in macrophages infected with *Yersinia*. Thus, this study reveals new insights into inflammasome regulation during *Yersinia* infection.

Recognition of microbial pathogens by the innate immune system is a crucial component of host defense. Pattern recognition receptors recognize conserved features of microbes, termed pathogen-associated molecular patterns (PAMPs), and mobilize host defenses against both extracellular and intracellular pathogens (1). Detection of extracellular PAMPs by Toll-like receptors (TLRs) or of cytosolic PAMPs by nucleotide-binding oligomerization domain leucine-rich repeat (LRR) receptors (NLRs) initiates cellular events important for clearance of pathogens, such as expression of proinflammatory cytokines or inflammasome formation (2, 3).

PAMPs and other danger signals associated with pathogens that access the host cytosol trigger the formation and activation of the inflammasome, a multioligomeric complex that serves as a molecular platform for the recruitment and activation of proinflammatory caspase-1 (4). Formation of the inflammasome is coordinated by protein-protein interactions between individual NLRs and in some cases an adaptor protein, adaptor protein apoptosis-associated speck-like protein containing a caspase activation and recruitment domain (ASC). Some inflammasomes (e.g., the NLRP3 inflammasome) require distinct signals for prim-

ing and activation. Induction of transcription downstream of TLR stimulation by a PAMP (signal 1) leads to the synthesis of NLRP3 and prointerleukin-1β (pro-IL-1β). The NLRP3 inflammasome is subsequently assembled and activated by a wide variety of stimuli (signal 2), such as pore-forming toxins or extracellular ATP (5, 6). In contrast, the NLRC4 inflammasome does not require a priming step and is more selective for activating stimuli such as bacterial flagellin and components of bacterial type III secretion systems (T3SS) (7, 8). While the regulation and composition of different inflammasomes are variable, they all have the ability to activate caspase-1. Caspase-1 activation by the inflammasome induces a form of cell death termed pyroptosis (9). In addition, the proinflammatory cytokines IL-1β and IL-18, synthesized as inactive precursors, rely on the activity of caspase-1 for their maturation and secretion from the host cell (4). The caspase-1-dependent processes of pyroptosis and cytokine secretion act in concert to promote innate immune responses, enabling clearance of invading pathogens. Thus, evasion of innate immune responses dependent on caspase-1 is an important strategy of pathogenic bacteria.

Pathogenic *Yersinia* species (*Yersinia pestis*, *Y. pseudotuberculosis*, and *Y. enterocolitica*) employ a contact-dependent T3SS for the delivery of *Yersinia* outer protein (Yop) effectors into the cytosol of infected host cells (10). Yop effectors function to modulate key host processes to promote *Yersinia* pathogenesis (11). Delivery of effector Yops requires the assembly of the T3SS injectisome on the bacterial surface and insertion of the YopB/D translocon into the plasma membrane of host cells. Consequences of membrane perturbation by the T3SS translocon are assembly of inflammasomes and activation of caspase-1 during the infection of macrophages by *Yersinia* (12, 13). However, Yop effectors counteract the activation of inflammasomes and caspase-1. Activation of caspase-1 by the T3SS translocon is mediated primarily by the NLRP3 inflammasome and is counteracted by the function of the effector YopK, which interacts with the translocon and prevents caspase-1 activation (14). Recently, a second effector, YopM, an LRR-containing protein that is required for *Yersinia* virulence (15, 16), has been shown to inhibit NLRP3 inflammasome formation and activation of caspase-1 (17).

YopM consists of an N-terminal secretion signal, followed by two α-helices that fold into an LRR region, which spans most of the protein (18). The YopM protein terminates in a short, unstructured but conserved C-terminal tail of 24 amino acids. Interestingly, YopM appears to be devoid of catalytic activity, and instead, this protein acts as a scaffold to bind multiple host proteins. YopM was found to bind two host kinases, protein kinase C-related kinase 2 (PRK2) and the 90-kDa ribosomal S6 kinase (RSK1), and increase their activity toward a heterologous substrate (19, 20). RSK1 binds to the C-terminal tail of YopM, and PRK2 binds to the LRR region (21, 22). How complexes of YopM/ RSK/PRK contribute to *Yersinia* virulence remains unknown. The LRR region and the C-terminal tail are both required for the virulence function of YopM (21, 22). Additionally, the C-terminal tail is required for the formation of high-molecular-weight complexes by YopM in macrophages (21). Each strain of *Yersinia* encodes one isoform of YopM, but there are a number of different isoforms found in the genus (23), and depending on the specific isoform, the LRR region contains between 13 and 21 repeats and the LRRs can be variable in sequence.

LaRock and Cookson presented evidence that YopM proteins containing 15 LRRs encoded by *Y. pseudotuberculosis* strain YPIII

and *Y. pestis* strain CO92 bind directly to caspase-1 to inhibit its activity (17). These two isoforms of YopM, as exemplified by YopM$^{\text{YPIII}}$, contain a consensus caspase-1 cleavage motif (Tyr-Leu-Thr-Asp or YLTD) present in the 10th LRR and appear to mimic pseudosubstrate caspase-1 inhibitors (17). YopM$^{\text{YPIII}}$ was shown to inhibit capsase-1 activity *in vitro*, to bind to the 10-kDa subunit of active caspase-1 in lysates of macrophages, and to inhibit the recruitment of caspase-1 to macromolecular complexes of NLRP3 (NLRP3 foci) in YPIII-infected macrophages (17). In contrast, a YopM$^{\text{YPIII}}$ variant in which the fourth position of the YLTD sequence was changed to A ($D_{271}A$) was defective in all of these activities (17). LaRock and Cookson proposed that YopM$^{\text{YPIII}}$ uses the YLTD sequence to bind directly to caspase-1 to inhibit its activity and sequester it, resulting in the formation of arrested or "pre-NLRP3 inflammasomes" (17). Importantly, the virulence defect of a YPIII *yopM* mutant was reversed in mice lacking caspase-1, indicating that YopM functions to inhibit capase-1-directed immune functions *in vivo* (17).

The findings of LaRock and Cookson (17) provide the first molecular understanding of how a YopM protein can inhibit host innate immune responses, yet they raise a number of important questions. For example, do YopM isoforms that lack the YLTD sequence (of which there are many among different *Yersinia* species and strains) also inhibit the activation of caspase-1? Is the C-terminal RSK1-binding tail of YopM, which is essential for its virulence function, also required to inhibit caspase-1? Does the LRR domain of YopM target other host proteins in addition to caspase-1 to inhibit the function of the NLRP3 inflammasome?

Here, we studied two distinct YopM isoforms, YopM^{32777} from *Y. pseudotuberculosis* 32777 and YopM$^{\text{KIM}}$ from *Y. pestis* KIM. The former contains 21 LRRs and lacks the YLTD sequence, while the latter contains 15 LRRs and the YLTD sequence in LRR 10. We demonstrate that both YopM isoforms inhibit the activation of caspase-1 in mice or macrophages infected with *Y. pseudotuberculosis*. In addition, using deletion variants of YopM$^{\text{KIM}}$, we provide evidence that both LRRs 6 to 15 and the C-terminal tail are necessary to inhibit the activation of caspase-1. Analysis of a YopM$^{\text{KIM}}$ $D_{271}A$ variant showed that the YLTD sequence is dispensable for the inhibition of caspase-1 activation in this isoform. We also identify the large scaffolding protein IQGAP1 (IQ motif-containing GTPase-activating protein 1) (24) as a novel interacting partner of the YopM$^{\text{KIM}}$ LRR domain and show that IQGAP1 is required for caspase-1 activation in macrophages infected with a *Y. pseudotuberculosis yopM* mutant. These results suggest that distinct YopM isoforms target different host proteins to inhibit caspase-1 activation and show that IQGAP1 is required for the activation of caspase-1 in macrophages infected with *Yersinia*.

RESULTS AND DISCUSSION

Sequence comparison of *Y. pestis* KIM and *Y. pseudotuberculosis* 32777 YopM proteins. Two well-studied YopM isoforms, YopM$^{\text{KIM}}$ and YopM^{32777}, contain 15 and 21 LRRs, respectively. Here, we have aligned the YopM^{32777} and YopM$^{\text{KIM}}$ sequences by using ClustalW (see Fig. S1 in the supplemental material). This analysis indicates that the N terminus and the C-terminal tail are conserved in YopM$^{\text{KIM}}$ and YopM^{32777} and the first two and last eight LRRs are well aligned (see Fig. S1). YopM^{32777} appears to have additional repeats within the region corresponding to LRRs 3 to 7 of YopM$^{\text{KIM}}$. To account for these additional LRRs in YopM^{32777}, they are numbered as subrepeats of LRRs 3, 5, and 7 of
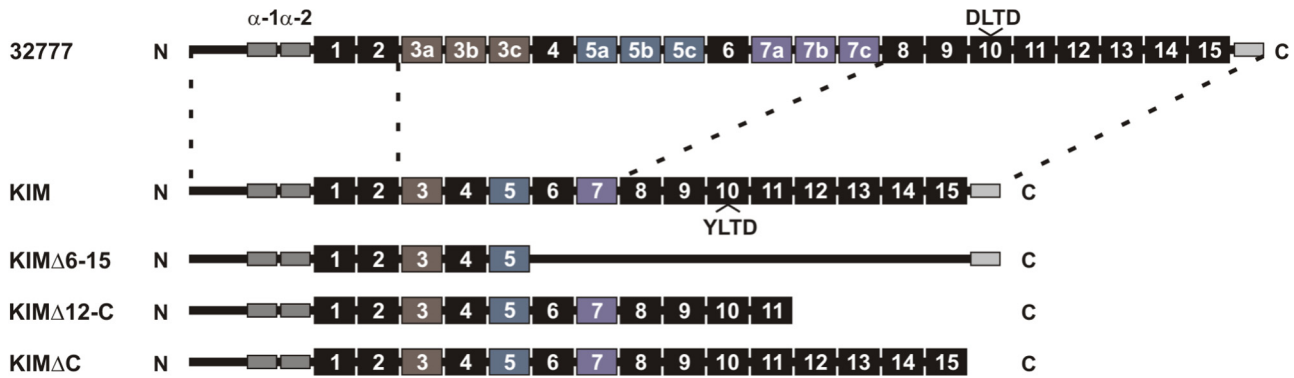
FIG 1 Primary-structure representation of the YopM isoforms and variants used in this study. Representations of YopM[32777], YopM[KIM], and three deletion variants of the KIM isoform are shown. N-terminal and C-terminal regions enclosed by dashed lines indicate the highest conservation between YopM[32777] and YopM[KIM], as determined by sequence alignment with ClustalW (see Fig. S1 in the supplemental material). The N-terminal gray rectangles correspond to the two α-helices, LRRs are represented by numbered boxes, and the conserved C-terminal tail is shown as a gray rectangle. Colored shading of boxes is used to indicate that additional LRRs in YopM[32777] are assigned numbers as subrepeats of LRRs 3, 5, and 7 of YopM[KIM]. The positions of the YLTD motif in LRR 10 of YopM[KIM] and the corresponding DLTD motif in LRR 10 of YopM[32777] are shown.

YopM[KIM] (see Fig. S1). The primary-structure alignment of YopM[KIM] and YopM[32777] by this convention is shown in Fig. 1. The YLTD motif in LRR 10 of YopM[KIM] is absent from the YopM[32777] isoform. Instead, YopM[32777] has the sequence DLTD (Fig. 1; see Fig. S1).

A *Y. pseudotuberculosis* 32777 *yopM* mutant is fully virulent in mice lacking caspase-1. *Y. pseudotuberculosis yopM* mutants are significantly attenuated in intravenous mouse models of infection (21, 22). LaRock and Cookson showed that the virulence defect of a YPIII *yopM* mutant was rescued in C57BL/6 mice lacking caspase-1 (17). We used *Caspase-1*^{−/−} C57BL/6 mice, which have been determined to be functionally *Caspase-11*^{−/−} as well (25) (here referred to as *Caspase-1/11*[−/−] mice), to investigate if the virulence of a 32777 *yopM* mutant would be restored in the absence of caspase-1. *Caspase-1/11*[−/−] mice were infected with equivalent numbers of CFU of 32777 or 32777Δ*yopM* (Table 1), and the time to death was monitored. As expected, 32777 was virulent in *Caspase-1/11*[−/−] mice following intravenous infection (Fig. 2, solid line). We previously showed that the 32777Δ*yopM* mutant is attenuated in C57BL/6 mice by intravenous challenge (22), a phenotype that was confirmed in independent experiments (data not shown). A reversal of the virulence defect of the 32777Δ*yopM* mutant was observed in *Caspase-1/11*[−/−] mice, as all of the mice succumbed to infection (Fig. 2, dotted line). The data are consistent with those of LaRock and Cookson (17) and

suggest that caspase-1-directed immune responses *in vivo* are responsible for the attenuation of *Y. pseudotuberculosis yopM* mutants. Moreover, these data point to inhibition of caspase-1 activation as a conserved function shared by distinct YopM isoforms. However, because the mice used are *Caspase-1/11*[−/−], the possibility cannot be ruled out that caspase-11-directed responses *in vivo* contribute to the attenuation of *Y. pseudotuberculosis yopM* mutants.

YopM[32777] inhibits caspase-1 activation in macrophages infected with *Y. pseudotuberculosis.* To obtain more direct evidence that YopM[32777] inhibits the activation of caspase-1, we infected lipopolysaccharide (LPS)-primed, bone marrow-derived macrophages (BMDMs) from C57BL/6 mice with 32777 or 32777Δ*yopM* and measured the activation of caspase-1. Caspase-1 activation was inhibited in C57BL/6 BMDMs infected with 32777 compared to that in 32777Δ*yopM*, as shown by Western blotting of macrophage lysates for cleaved (10-kDa) caspase-1 (Fig. 3A, compare lanes 1 and 5). Infection with a 32777Δ*yopK* mutant (Table 1) was used as a positive control for caspase-1 cleavage (Fig. 3A, lane 9). Additionally, unlike 32777, the 32777Δ*yopM* strain failed to inhibit IL-1β secretion (Fig. 3B) or pyroptosis (Fig. 3C), as determined by enzyme-linked immunosorbent assay (ELISA) or lactate dehydrogenase (LDH) release, respectively. Activation of caspase-1 by 32777Δ*yopM* required a functional T3SS, as caspase-1 was not activated when BMDMs were infected with a

**TABLE 1** *Y. pseudotuberculosis* strains used in this study

| Strain	Relevant characteristic(s)	Reference
32777	Wild-type serogroup O1 strain	41
32777Δ*yopM*	Δ*yopM*	22
32777Δ*yopK*	Frame-shift mutation in *yopK*	This study
32777Δ*yopMyopB*	Δ*yopM*, in-frame deletion of *yopB* (nucleotides 496–774)	This study
32777Δ*yopM*/pMMB67EH	Δ*yopM* containing empty vector	22
32777Δ*yopM*/pYopM[KIM]	Δ*yopM* containing pMMB67EH expressing YopM[KIM] under control of native promoter	22
32777Δ*yopM*/pYopM[KIM]Δ6-15	Δ*yopM* containing pMMB67EH expressing YopM[KIM] missing LRRs 6–15	22
32777Δ*yopM*/pYopM[KIM]Δ12-C	Δ*yopM* containing pMMB67EH expressing YopM[KIM] missing LRRs 12–15 and C terminus	This study
32777Δ*yopM*/pYopM[KIM]ΔC	Δ*yopM* containing pMMB67EH expressing YopM[KIM] missing C terminus	22
32777Δ*yopM*/pYopM[KIM] D[271]A	Δ*yopM* containing pMMB67EH expressing YopM[KIM] with D[271]A amino acid substitution	This study
32777/pGFP	Contains p67GFP3.1	32
32777Δ*yopM*/pGFP	Δ*yopM* containing p67GFP3.1	This study
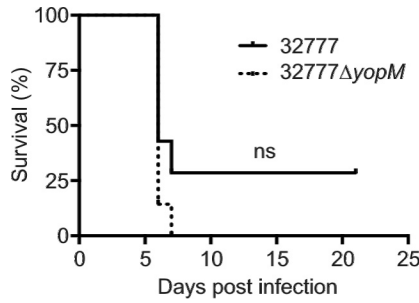
FIG 2 Survival assay of *Caspase-1/11−/−* mice infected with *Y. pseudotuberculosis* 32777 or 32777Δ*yopM*. *Caspase-1/11−/−* mice were infected intravenously via tail vein injection with approximately 1,500 CFU of *Y. pseudotuberculosis* 32777 or 32777Δ*yopM*, and time to death was monitored for 21 days. Results are pooled from two independent experiments with three or four mice per group (*n* = 7). The difference between survival curves was not significant (ns), as determined by log rank test.

32777Δ*yopMyopB* mutant (Table 1; see Fig. S2A in the supplemental material), as measured by Western blotting for cleaved caspase-1 (see Fig. S2B) and ELISA for secreted IL-1β (see Fig. S2C). Because caspase-11 can contribute to NLRP3-dependent activation of caspase-1 in response to cytosolic LPS (25, 26), we examined the role of caspase-11 in the response of BMDMs to infection with the 32777Δ*yopM* mutant. BMDMs from *Caspase-1−/−*, *Caspase-11−/−*, or *Caspase-1/11−/−* mice were infected and analyzed as described above. We observed similar amounts of cleaved caspase-1 in C57BL/6 and *Caspase-11−/−* BMDMs infected with 32777Δ*yopM* or 32777Δ*yopK* (Fig. 3A, compare lanes 5 and 8 and lanes 9 and 12). Likewise, the absence of caspase-11 did not significantly decrease the levels of secreted IL-1β in BMDMs infected with 32777Δ*yopM* (Fig. 3B). Interestingly, pyroptosis was partially caspase-11 dependent in BMDMs infected with the *yopM* mutant (Fig. 3C). As expected, IL-1β secretion (Fig. 3B) and pyroptosis (Fig. 3C) were at background levels in *Caspase-1−/−* and *Caspase-1/11−/−* BMDMs infected with 32777Δ*yopM*. The data show that YopM³²⁷⁷⁷ inhibits caspase-1 activation, demonstrating that this activity is not restricted to the 15 LRR isoforms that contain a YLTD motif. In addition, the data show that caspase-11 is not required for the activation of caspase-1 in macrophages infected with a *Y. pseudotuberculosis yopK* or *yopM* mutant but does contribute to pyroptosis in the latter case.

Differential binding of caspase-1 by YopM^KIM and YopM³²⁷⁷⁷. LaRock and Cookson showed that purified YopM^YPIII bound to cleaved caspase-1 in lysates derived from BMDMs infected with the YPIII *yopM* mutant (17). Because YopM^KIM and YopM³²⁷⁷⁷ both inhibited the activation of caspase-1, we wanted to determine if both proteins bind to cleaved caspase-1. To investigate the binding of YopM^KIM and YopM³²⁷⁷⁷ to caspase-1, these proteins were purified as fusions to glutathione *S*-transferase (GST) and incubated with lysates of BMDMs treated with LPS and ATP to activate caspase-1. Western blotting was used to detect the binding of caspase-1 or RSK1 to the GST-YopM fusion proteins or GST alone as a control. As shown in Fig. 4A, GST-YopM^KIM, but not GST, bound to procaspase-1 (50 kDa), as well as RSK1 (compare lanes 6 and 3). Weak binding of cleaved caspase-1 to GST-YopM^KIM was also detected (Fig. 4A, lane 6). Interestingly, we did not detect binding of procaspase-1 or cleaved caspase-1 to GST-
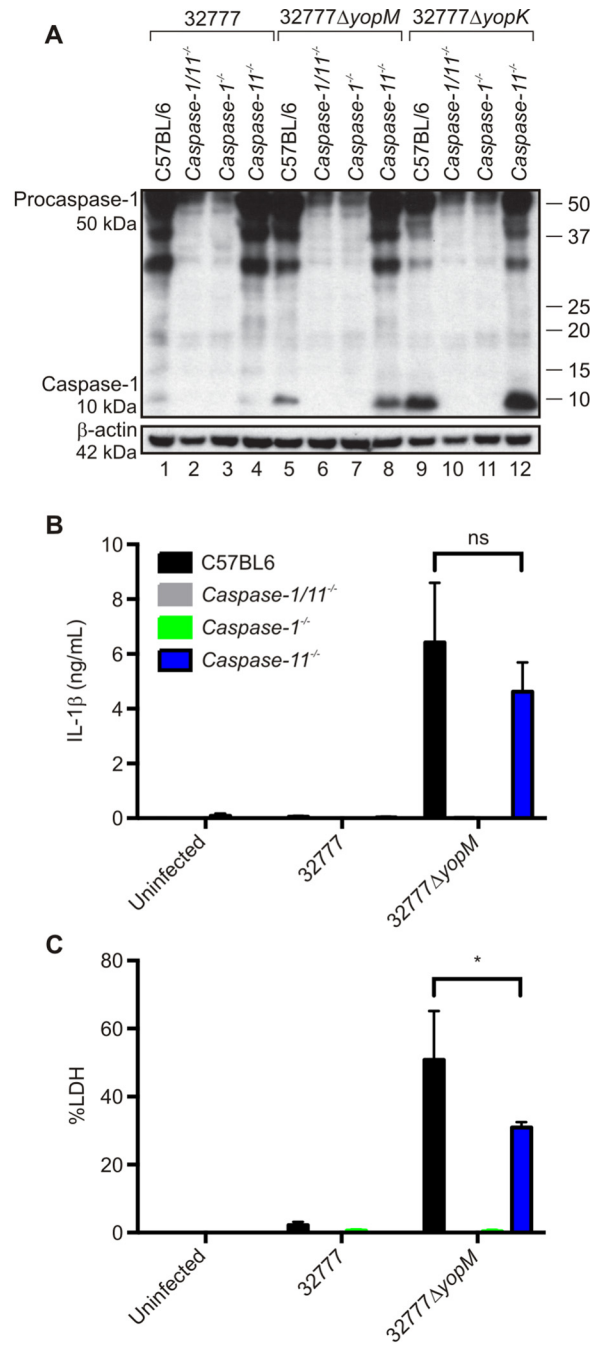
FIG 3 Measurement of caspase-1 activation in C57BL/6, *Caspase-1−/−*, *Caspase-11−/−*, or *Caspase-1/11−/−* mouse macrophages infected with *Y. pseudotuberculosis*. BMDMs from wild-type C57BL/6, *Caspase-1−/−*, *Caspase-11−/−*, or *Caspase-1/11−/−* mice were primed with 100 ng/ml LPS for 18 h and left uninfected or infected with 32777, 32777Δ*yopM*, or 32777Δ*yopK* at an MOI of 30. (A) After a 90-min infection, lysates were processed and subjected to Western blotting with an antibody against caspase-1. β-Actin was used as a loading control. Positions of 50-kDa procaspase-1, the cleaved 10-kDa caspase-1 subunit, and 42-kDa β-actin are shown on the left, and molecular size standards are shown on the right. (B) Supernatants were collected at 90 min postinfection, and secreted IL-1β was measured by ELISA. (C) Levels of cytotoxicity were measured by quantification of percent LDH release. The data in panels B and C are average values ± the standard errors of the means from three independent experiments. By two-way ANOVA comparing the C57BL/6 group to the *Caspase-11−/−* group infected with 32777Δ*yopM*, *P* < 0.05 (*).
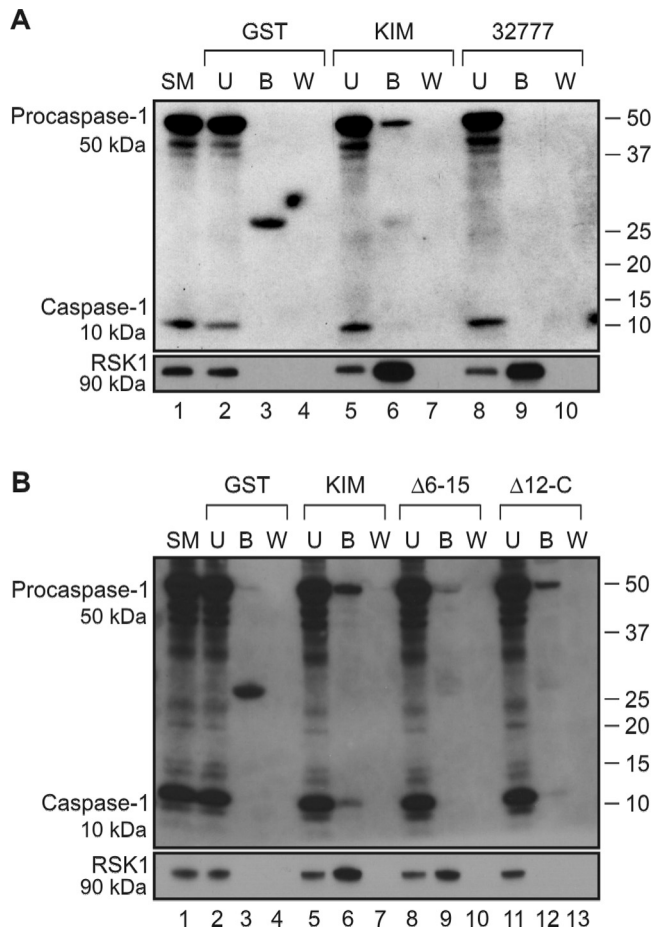
FIG 4 Interaction of host proteins with the GST-YopM^{32777}, GST-YopM^{KIM}, or GST-YopM^{KIM} deletion variant by pulldown assay. Ten micrograms of GST, GST-YopM^{KIM}, or the indicated GST-YopM^{KIM} deletion variant was loaded onto GST-Bind Sepharose beads and subsequently incubated with lysates prepared from C57BL/6 BMDMs activated by treatment with LPS and ATP. Proteins bound to the beads were eluted, resolved by SDS-PAGE, and detected by Western blotting with antibodies to caspase-1 or RSK1. (A) Western blot pulldown assay of interaction of GST or the GST-YopM^{KIM} or GST-YopM^{32777} fusion protein with caspase-1 or RSK1. (B) Western blot pulldown assay of interaction of GST, GST-YopM^{KIM} or GST-YopM^{KIM} deletion variant with caspase-1 or RSK1. SM, starting material; U, unbound; B, bound; W, wash. The positions of 50-kDa procaspase-1, the cleaved 10-kDa caspase-1 subunit, and 90-kDa RSK1 are shown on the left, and molecular size standards are shown on the right.

YopM^{32777} (Fig. 4A, lane 9). These data suggest that sequence differences account for the differential binding of YopM^{KIM} and YopM^{32777} to caspase-1. We previously constructed a series of deletion variants of YopM^{KIM} missing different numbers of LRRs or the C terminus (Fig. 1) (22). We used GST fusions of two of the YopM^{KIM} deletion variants (Δ6-15 and Δ12-C) to delineate the regions of the protein required for binding to procaspase-1 and cleaved caspase-1. As shown in Fig. 4B, GST-YopM^{KIM} (lane 6) and the Δ12-C variant (lane 12) bound to both procaspase-1 and cleaved caspase-1, while the Δ6-15 variant (lane 9) failed to interact with either protein. As expected, the Δ12-C variant failed to bind RSK1, while the Δ6-15 variant retained this activity (Fig. 4B, compare lanes 12 and 9). Thus, binding to both procaspase-1 and cleaved caspase-1 requires LRRs 6 to 11 of YopM^{KIM}. Taken to-

gether, these data demonstrate differential binding of caspase-1 by YopM^{KIM} and YopM^{32777} *in vitro*, even though both proteins inhibit the activation of caspase-1 *in vivo*. The use of a different isoform (YopM^{YPIII}) or a different stimulus (infection) to activate caspase-1 in macrophages could explain why LaRock and Cookson failed to detect binding of procaspase-1 in their experiments (17).

LRRs 6 to 15 and the C terminus of YopM^{KIM} are necessary for inhibition of activation of caspase-1. To investigate which domains of YopM^{KIM} are required to inhibit the activation of caspase-1 in macrophages, the Δ6-15, Δ12-C, and ΔC deletion variants (Fig. 1) (22) and the wild-type protein were expressed in 32777Δ*yopM* under the control of the native YopM promoter (Table 1). A Yop secretion assay confirmed that the expression and stability of the YopM^{KIM} deletion variants were similar to those of the wild-type protein (Fig. 5A). These strains, as well as the 32777 and 32777Δ*yopM* controls, were subsequently used to infect C57BL/6 BMDMs to assess whether the LRR region of the protein is sufficient to inhibit the activation of caspase-1. As expected, 32777Δ*yopM* was defective for inhibition of IL-1β secretion in BMDMs and this phenotype was complemented by the expression of YopM^{KIM} (Fig. 5B). BMDMs infected with the strain expressing the Δ6-15 variant secreted an amount of IL-1β similar to that secreted by those infected with 32777Δ*yopM* (Fig. 5B). Interestingly, strains expressing either the Δ12-C or the ΔC variant failed to inhibit IL-1β secretion (Fig. 5B and C), suggesting that the C terminus of YopM^{KIM} is important for inhibition of caspase-1 activation. Taken together, the data reveal that both the region comprising LRRs 6 to 15 and the C-terminal tail of YopM^{KIM} are required for inhibition of the activation of caspase-1.

A YLTD motif in YopM^{KIM} is not required to inhibit the activation of caspase-1. Mutation of the aspartic acid residue in the YLTD motif in YopM^{YPIII} to an alanine ($D_{271}A$) abrogated its ability to bind to and inhibit the activation of caspase-1 (17). We introduced the identical mutation into the gene encoding YopM^{KIM} to assess if the YLTD motif is required for the *Y. pestis* protein to inhibit the activation of caspase-1. Figure 6A shows that the YopM^{KIM} $D_{271}A$ protein is produced by 32777Δ*yopM* at the same levels as the wild-type protein in a Yop secretion assay (compare lanes 2 and 3). Surprisingly, when we infected C57BL/6 BMDMs with 32777Δ*yopM* expressing the YopM^{KIM} $D_{271}A$ variant, both caspase-1 cleavage (Fig. 6B, lane 5) and IL-1β secretion (Fig. 6C) were inhibited, arguing that the YLTD motif in YopM^{KIM} is not required to inhibit the activation of caspase-1.

YopM^{KIM} interacts with IQGAP1. To determine if novel host proteins bind to YopM^{KIM}, pulldown assays with LPS-primed C57BL/6 BMDM lysates and GST, GST-YopM^{KIM}, or a GST-YopM^{KIM} Δ6-15 or Δ12-C deletion variant were carried out. Bound proteins were, eluted, resolved by sodium dodecyl sulfate-polyacrylamide gel electrophoresis (SDS-PAGE), and visualized by silver staining. As shown in Fig. 7A, an ~200-kDa protein bound to GST-YopM^{KIM} (lane 2) and the Δ12-C variant (lane 5) but not to GST (lane 1) or the Δ6-15 variant (lane 4). The ~200-kDa protein was not detected when the pulldown was done with GST-YopM^{KIM} in lysis buffer alone (Fig. 7A, lane 3), suggesting that it was specific to the macrophage lysate. The region of the gel containing the ~200-kDa protein was excised and subjected to mass spectrometry analysis, and the corresponding protein was identified as the murine scaffolding protein IQGAP1 (24). Inter-
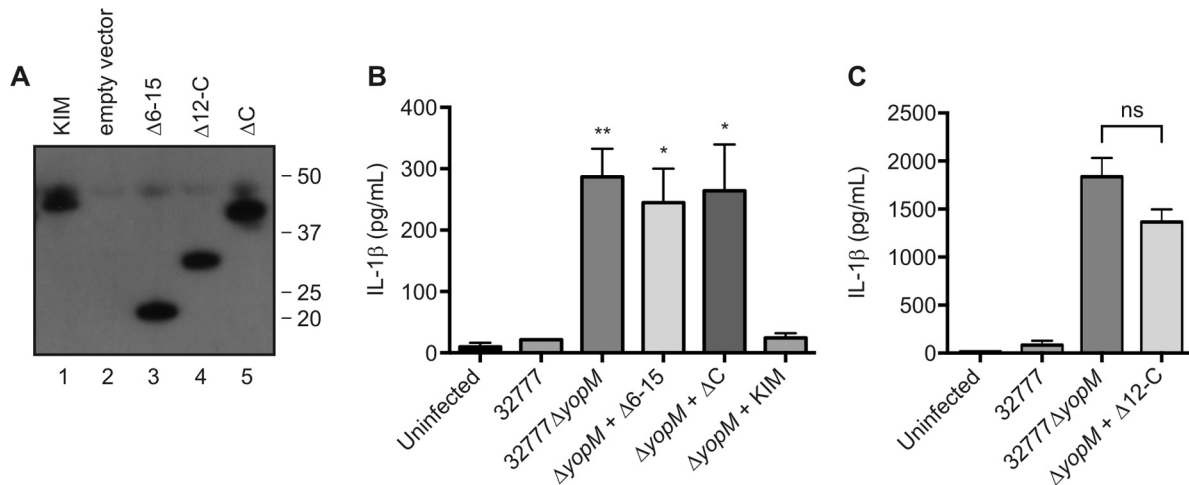
FIG 5 Analysis of YopM^{KIM} deletion variant stability and inhibition of IL-1β secretion in macrophages infected with *Y. pseudotuberculosis*. (A) Stability of YopM^{KIM} deletion variants as shown by a Yop secretion assay and Western blotting with a monoclonal antibody that recognizes an epitope in the N-terminal domain of the protein. The 32777$\Delta yopM$ strain encoding YopM^{KIM} (KIM), the empty vector, or the indicated deletion variant was used for the Yop secretion assay, and samples of secreted proteins analyzed by Western blotting were normalized by the OD of the bacterial cultures. (B and C) C57BL/6 BMDMs primed with 100 ng/ml LPS for 18 h were left uninfected or infected with the indicated strains of *Y. pseudotuberculosis* at an MOI of 30. Supernatants were collected at 90 min postinfection and analyzed by ELISA to quantify levels of secreted IL-1β. The data are average values $\pm$ the standard errors of the means from three or four independent experiments. In panel B, a one-way ANOVA was used for comparisons with the $\Delta yopM$ + KIM group. *, $P < 0.05$; **, $P < 0.01$; ns, not significant.

estingly, IQGAP1 has previously been identified as a target of the type III effector proteins Ibe of enteropathogenic *Escherichia coli* (27) and SseI of *Salmonella enterica* serovar Typhimurium (28). In these cases, IQGAP1 was important for pedestal formation in epithelial cells by *E. coli* (27) or inhibition of macrophage and dendritic cell migration by *S.* Typhimurium (28). To verify the results obtained by mass spectrometry, samples from pulldown experiments were analyzed by Western blotting with an antibody against IQGAP1. As shown in Fig. 7B, IQGAP1 bound specifically to GST-YopM^{KIM} (lane 5) and the Δ12-C variant (lane 11). These data indicate that YopM^{KIM} interacts with IQGAP1 and that LRRs 6 to 11 are required for this interaction. Similar experiments performed with GST-YopM^{32777} showed that IQGAP1 does not bind to this isoform (data not shown). It remains to be determined whether the interaction of IQGAP1 and YopM^{KIM} is direct or mediated by a cofactor.

IQGAP1 is important for caspase-1 activation in macrophages infected with *Y. pseudotuberculosis*. The interaction between YopM^{KIM} and the scaffolding protein IQGAP1 suggested to us that the latter protein might be important for the activation of caspase-1 in macrophages infected with *Yersinia*. We assessed the role of IQGAP1 in the activation of caspase-1 by infecting LPS-primed BMDMs from wild-type 129 mice or 129 *Iqgap1$^{-/-}$* mice with *Y. pseudotuberculosis* and measuring caspase-1 cleavage and IL-1β secretion. There was less cleavage of caspase-1 in *Iqgap1$^{-/-}$* BMDMs, than in BMDMs from 129 wild-type controls when they were infected with 32777$\Delta yopM$ (Fig. 8A, compare lanes 8 and 3). Additionally, there was significantly less secretion of IL-1β in *Iqgap1$^{-/-}$* BMDMs than in the wild-type controls when they were infected with 32777$\Delta yopM$ (Fig. 8B). We noted that secretion of IL-1β by *Iqgap1$^{-/-}$* BMDMs infected with 32777$\Delta yopM$ was not completely abolished but rather severely decreased (Fig. 8B), indicating that IQGAP1 is important but not essential for activation of caspase-1 under these conditions. Interestingly, in response to
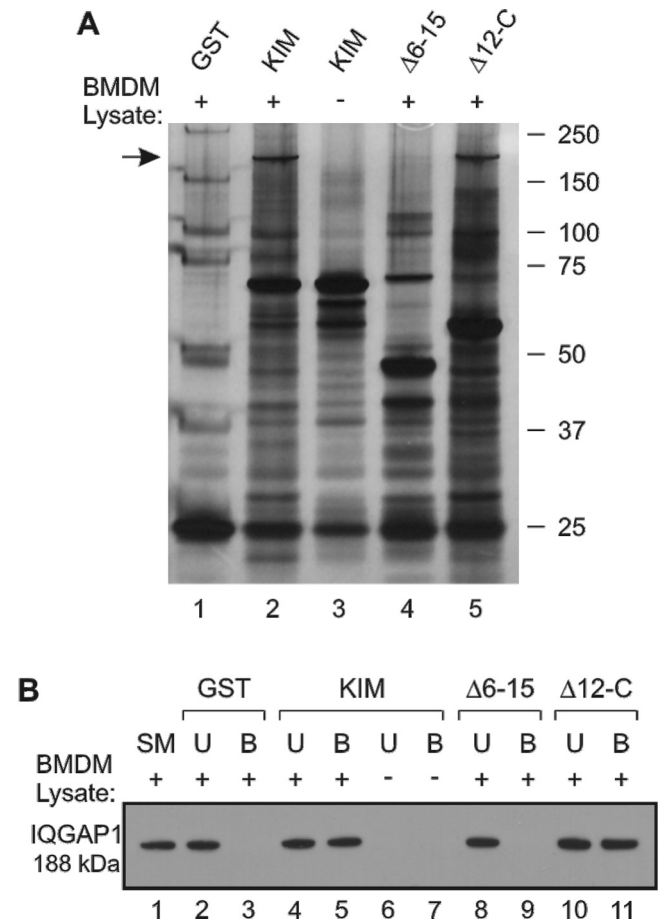
extracellular ATP, a canonical activator of the NLRP3 inflammasome, there was no noticeable difference in the amount of cleaved caspase-1 (Fig. 8A, compare lanes 5 and 10) or secreted IL-1β (Fig. 8B) between 129 and *Iqgap1$^{-/-}$* BMDMs. Failure to secrete IL-1β was not due to a defect of YopB/D translocon insertion in *Iqgap1$^{-/-}$* BMDMs, as there was no noticeable difference in YopM translocation between 129 and *Iqgap1$^{-/-}$* BMDMs (Fig. 8C, compare lanes 1 and 4 and lanes 3 and 6). Additionally, there was no detectable difference between 129 and *Iqgap1$^{-/-}$* BMDMs in the kinetics of their cell rounding response to effectors that disrupt the actin cytoskeleton (data not shown), indicating that IQGAP1 is not required for translocation. These data suggest that IQGAP1 is specifically important for activation of the NLRP3 inflammasome in macrophages during *Yersinia* infection but dispensable for other NLRP3-dependent stimuli that lead to caspase-1 activation. To determine if IQGAP1 is required for the formation of macromolecular complexes of NLRP3 or a later step in inflammasome assembly, we used immunofluorescence microscopy to detect NLRP3 focus formation in 129 or *Iqgap1$^{-/-}$* BMDMs infected with *Y. pseudotuberculosis*. NLRP3 foci were not detected in uninfected 129 BMDMs but were detected in these cells infected with 32777 (see Fig. S3 in the supplemental material). In addition, NLRP3 foci formed in 129 and *Iqgap1$^{-/-}$* BMDMs infected with 32777$\Delta yopM$ (see Fig. S3), suggesting that IQGAP1 functions downstream of NLRP3 activation. These results are consistent with the idea that YopM inhibits the recruitment of procaspase-1 to NLRP3 preinflammasomes (17) through targeting of IQGAP1.

Summary. We have extended the results of LaRock and Cookson (17) by showing that (i) distinct YopM isoforms inhibit the activation of caspase-1, (ii) the LRR region and C-terminal tail are both required for this activity, and (iii) YopM^{KIM} binds to IQGAP1, which we have identified as a novel regulator of inflammasome function in macrophages. A model of the activation of
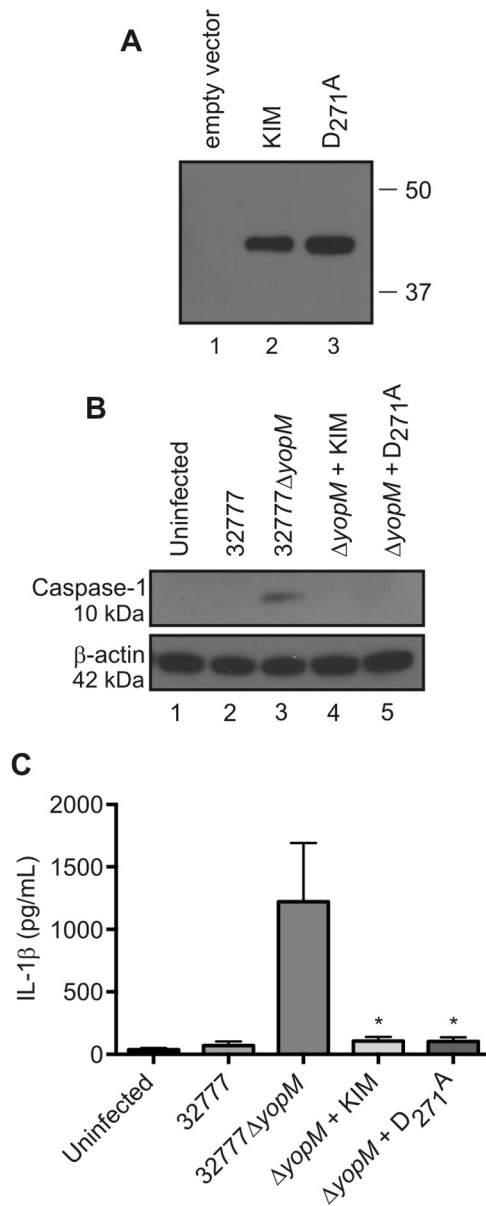
FIG 6 Analysis of YopM^{KIM} D$_{271}$A stability and the ability to inhibit the activation of caspase-1 in macrophages infected with *Y. pseudotuberculosis*. (A) Stability of the YopM^{KIM} D$_{271}$A variant as shown by a Yop secretion assay with a monoclonal antibody directed against the N terminus of YopM. 32777Δ*yopM* with the empty vector or expressing YopM^{KIM} or YopM^{KIM} D$_{271}$A was used for the Yop secretion assay, and samples were normalized by the OD of the bacterial cultures. (B and C) BMDMs primed with 100 ng/ml LPS for 18 h were left uninfected or infected at an MOI of 30 with 32777, 32777Δ*yopM*, or 32777Δ*yopM* expressing YopM^{KIM} or YopM^{KIM} D$_{271}$A. (B) At 90 min postinfection, BMDM lysates were collected and Western blotted for cleaved the 10-kDa caspase-1 subunit. β-Actin was used as a loading control (C) Supernatants were analyzed by ELISA for secreted IL-1β. The data in panel C are average values ± the standard errors of the means from three independent experiments. *, $P < 0.05$ (compared with the 32777Δ*yopM* group by one-way ANOVA).

FIG 7 Identification of IQGAP1 as a novel binding partner of YopM^{KIM}. Ten micrograms of GST, GST-YopM^{KIM}, or the GST-YopM^{KIM} deletion variant indicated was loaded onto GST-Bind Sepharose beads and subsequently incubated with lysates prepared from LPS-primed C57BL/6 BMDMs or lysis buffer alone. Unbound proteins were removed, the beads were washed, and bound proteins were eluted and resolved by SDS-PAGE. (A) Silver staining detection of eluted proteins after incubation with BMDM lysate (lanes 1, 2, 4, and 5) or lysis buffer alone (lane 3). The arrow indicates an ~200-kDa protein that was excised from the gel, fragmented by trypsin digestion, subjected to analysis by LC-MS/MS, and identified as murine IQGAP1. (B) Western blot analysis of samples (starting material [SM], unbound [U], and bound [B]) from pull-down assays with BMDM lysate (lanes 1 to 5 and 8 to 11) or lysis buffer alone (lanes 6 and 7) with an antibody against IQGAP1 (188 kDa).

the NLRP3 inflammasome in macrophages in response to *Yersinia* infection and mechanisms of caspase-1 inhibition by YopM is presented in Fig. 9. We speculate that translocon insertion and effector translocation generate distinct signals that sequentially stimulate the formation of NLRP3 preinflammasomes (signal 2) and recruitment of caspase-1 to NLRP3 foci (signal 3) to complete inflammasome formation (Fig. 9). Translocon insertion could generate signal 2 by causing ion fluxes or other types of plasma membrane perturbation, while the entry of effectors, or PAMPs, into the cytosol may generate signal 3 (Fig. 9). Our data show that the C-terminal tail and LRRs 6 to 15 of YopM^{KIM} are required to inhibit caspase-1 activation (mechanism A in Fig. 9). Preliminary results of translocation assays indicate that the Δ6-15 and Δ12-C variants exhibit reduced translocation and/or stability in infected macrophages, compared to the ΔC variant and YopM^{KIM} (data not shown). Therefore, the Δ6-15 and Δ12-C variants may be defective for inhibition of caspase-1 activation, in part because of reduced translocation or stability. The requirement for the C terminus, which is necessary for virulence *in vivo* (21, 22), may reflect
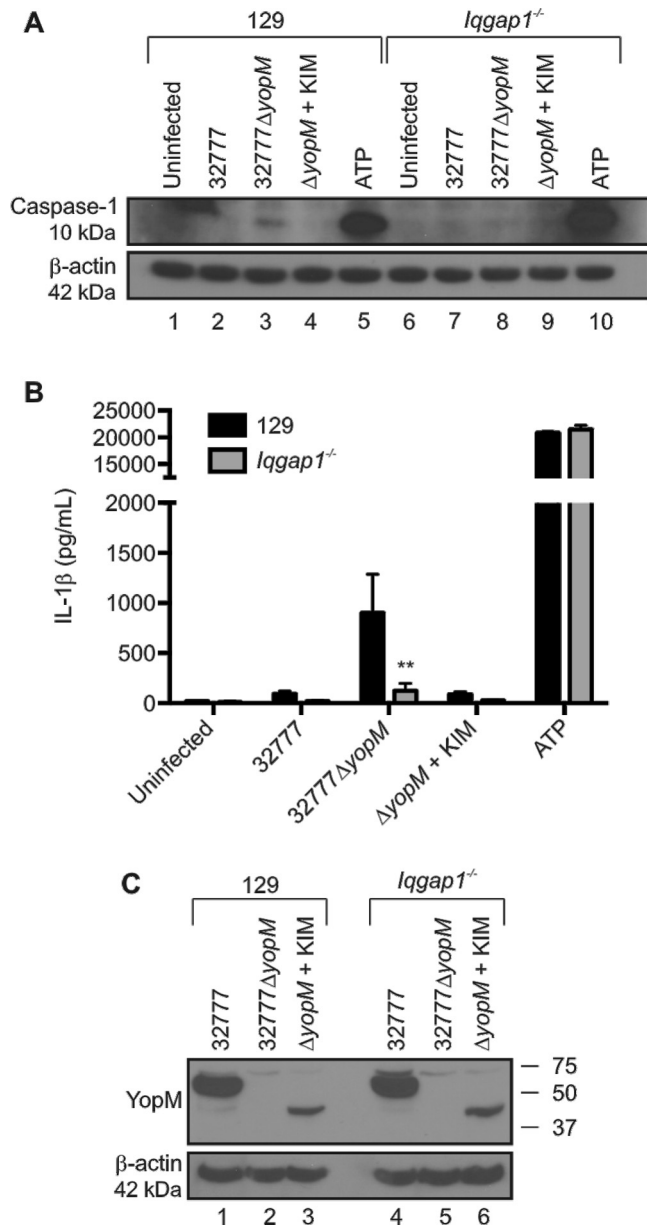
FIG 8 Measurement of caspase-1 activation and YopM translocation in 129 or *Iqgap1⁻/⁻* mouse macrophages infected with *Y. pseudotuberculosis*. BM-DMs from 129 or *Iqgap1⁻/⁻* mice were primed with 100 ng/ml LPS for 18 h and left uninfected or infected for 90 min at an MOI of 30 with the indicated strains of *Y. pseudotuberculosis*. Alternatively, 129 or *Iqgap1⁻/⁻* BMDMs were treated with 100 ng/ml LPS for 4 h and then exposed to 2.5 mM ATP for 1 h to serve as a positive control for activation of caspase-1. (A) Lysates were collected and processed by Western blotting for cleaved caspase-1 or β-actin. (B) Supernatants were collected and analyzed by ELISA to quantify levels of secreted IL-1β. (C) Lysates were collected and processed by Western blotting for YopM or β-actin. The data in panel B are average values ± the standard errors of the means from three independent experiments. **, $P < 0.01$ (compared to 32777Δ*yopM*-infected 129 BMDMs by one-way ANOVA).

its role in the multimerization of YopM (Fig. 9) (21). It will be important to determine if RSK1, by promoting YopM multimerization or exhibiting kinase activity, has an important role in the inhibition of caspase-1 cleavage. We suggest that LRRs 6 to 11 in YopM^KIM are essential for inhibition of caspase-1 activation be-

cause they target the protein to IQGAP1 (Fig. 9). It is unclear how IQGAP1 functions in this novel capacity to activate caspase-1, but as shown in Fig. 9, it is possible that it is important to transmit signal 3 for the recruitment of procaspase-1 to NLRP3 preinflammasomes. Using immunofluorescence microscopy we were unable to detect the localization of IQGAP1 to NLRP3 foci in macrophages infected with *yopM* mutant *Y. pseudotuberculosis* (data not shown). IQGAP1 is a ubiquitously expressed scaffolding protein that plays a role in diverse cellular processes (29, 30), and although it does not appear to localize to NLRP3 foci, it does interact with multiple host proteins, including Rho GTPases and kinases (29), that could regulate inflammasome assembly. IQGAP1 could also control caspase-1 cleavage by regulating actin organization or transcription, as these processes are known to be important for activation of the NLRP3 inflammasome. It remains to be determined if and how YopM^KIM inhibits IQGAP1 function. Preliminary experiments show that steady-state levels of IQGAP1 are unaffected by the presence of YopM^KIM in macrophages infected with *Y. pseudotuberculosis*. A final issue that remains to be addressed is the role of the YLTD motif (17), which appears to be required for YopM^YPIII to inhibit procaspase-1 recruitment to NLRP3 foci, activation of caspase-1 in macrophages, and caspase-1 activity *in vitro* (mechanism B, Fig. 9), but is dispensable for YopM^32777 and YopM^KIM to inhibit the activation of caspase-1 in macrophages. YopM^YPIII and YopM^KIM are 99.5% identical at the amino acid level (17), making it unlikely that amino acid differences between these isoforms could explain the different results obtained. It seems more likely that in 15-LRR YopM isoforms that contain a YLTD motif, the sequence naturally plays a cryptic role in the inhibition of caspase-1, and the specific *in vitro* experimental conditions used by LaRock and Cookson uncovered an unusually important role for this motif. A *Y. pseudotuberculosis* strain expressing a 15-LRR isoform (YopM^IP2666) in which repeats 10 to 11 were deleted was fully virulent in a mouse model of infection (21), arguing that the YLTD motif is dispensable for caspase-1 inhibition *in vivo*. A better understanding of how different YopM isoforms inhibit the activation of caspase-1 in macrophages is likely to lead to new insights into how inflammasomes are regulated and promote host protection against microbial infections.

MATERIALS AND METHODS

Bacterial strains and plasmids. A description of the *Y. pseudotuberculosis* strains used in this study is provided in Table 1. A frame-shift mutation was introduced into *yopK* in 32777 as previously described (31), generating 32777Δ*yopK*. An in-frame deletion of *yopB* was constructed in the 32777Δ*yopM* background as previously described (31), generating 32777Δ*yopMyopB*. Vectors encoding YopM^KIM and YopM^KIM deletion variants under the control of the native YopM promoter were generated in pMMB67EH and used to transform 32777Δ*yopM* as previously described (22). The pYopM^KIM Δ12-C vector was reconstructed in this study by the same approach and was analyzed independently of the other deletion variants, as shown in Fig. 5C. The vector pYopM^KIM D₂₇₁A was constructed as follows. The $D_{271}A$ codon change was introduced into pYopM^KIM with the QuikChange site-directed mutagenesis kit (Agilent) and primers described in reference 17. The plasmids constructed in this study were verified by sequencing. 32777 and 32777Δ*yopM* were transformed with a plasmid expressing green fluorescent protein (GFP) by mating with *E. coli* s17-1λpir harboring p67GFP3.1 as previously described (32). For infection of BMDMs, *Y. pseudotuberculosis* strains were grown overnight in Luria broth (LB) at 28°C. The following day, cultures were diluted 1:40 in LB containing 20 mM MgCl₂ and 20 mM sodium oxalate, grown at 28°C for 1 h, and then shifted to 37°C for 2 h. For analysis
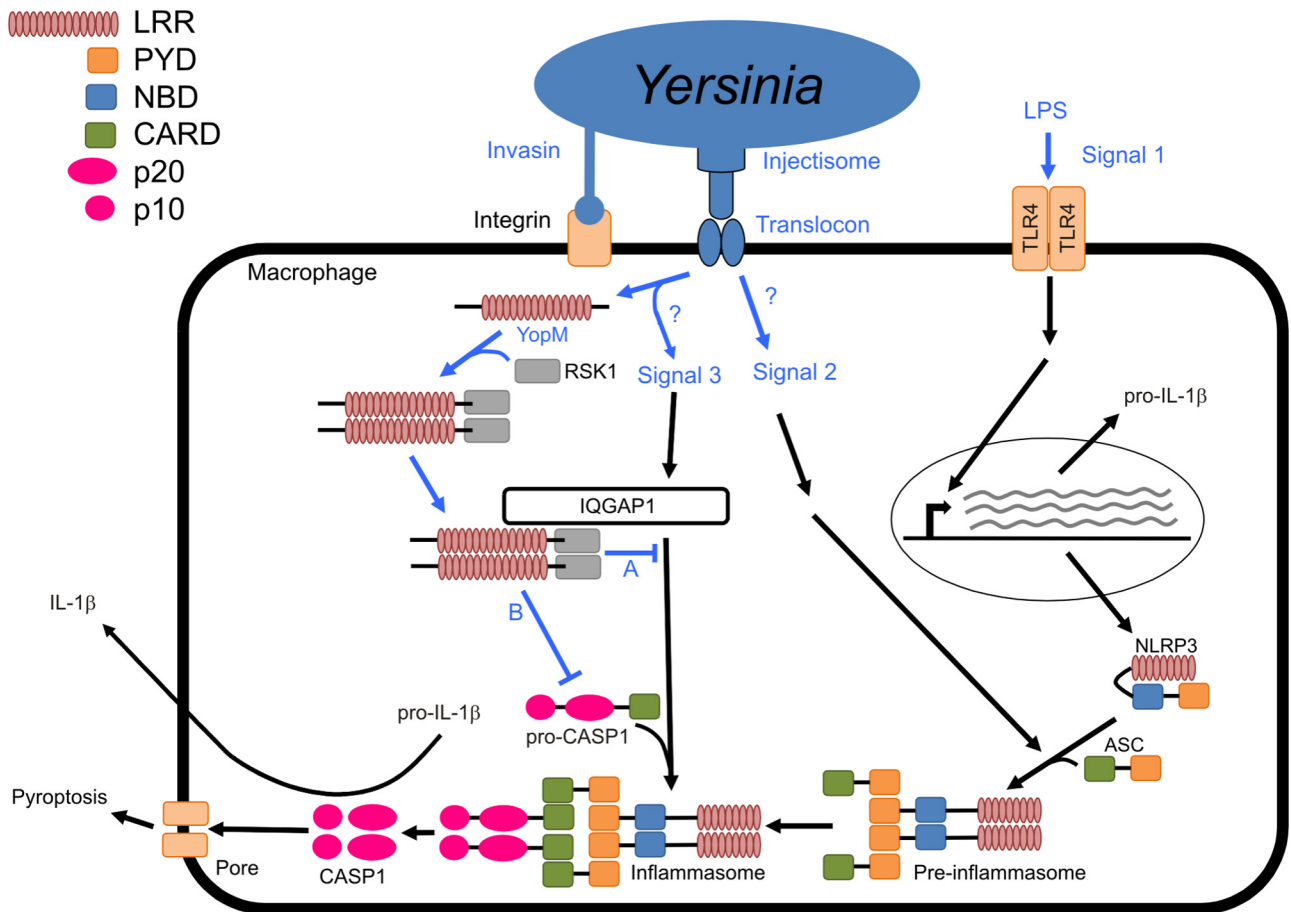
FIG 9 Model of NLRP3 inflammasome activation in *Yersinia*-infected macrophages and mechanisms of caspase-1 inhibition by YopM. LPS activates TLR4 (signal 1), resulting in transcription and synthesis of NLRP3 and pro-IL-1β. Binding of yersiniae to macrophage β1-integrin via invasin allows injectisome activation and translocon insertion into the plasma membrane. Translocon insertion is proposed to activate signal 2, leading to activation of NLRP3 and assembly with ASC into preinflammasomes. Translocation of Yop effectors, including YopM, is proposed to activate signal 3, which is sensed by IQGAP1, resulting in the recruitment of procaspase-1 into NLRP3/ASC foci to form inflammasomes, in which active caspase-1 is generated. YopM associates with RSK1 via its C-terminal tail and multimerizes. YopM^{KIM} binds to IQGAP1 via its LRRs and inhibits signal 3 by an unknown mechanism (A). YopM^{KIM}'s YLTD motif may also bind directly to procaspase-1 and active caspase-1 (B) to inhibit its recruitment to inflammasomes and its activity. Abbreviations: PYD, pyrin domain; NBD, nucleotide-binding oligomerization domain; CARD, caspase activation and recruitment domain; p20, 20-kDa subunit of active caspase-1; p10, 10-kDa subunit of active caspase-1.

of secreted Yops, yersiniae were diluted and grown as described above, except at 28°C for 2 h, followed by a temperature shift to 37°C for 4 h.

Mouse infections. *Y. pseudotuberculosis* cultures were grown overnight in LB at 28°C, washed twice with phosphate-buffered saline (PBS), and suspended to approximately 1.5×10^4 CFU/ml. A volume of 100 μl from this suspension was delivered by tail vein injection into *Caspase-1/11$^{-/-}$* mice (33) (a gift from Adrianus van der Velden, Stony Brook University). Time to death was monitored for 21 days, at which point the remaining mice were euthanized. All mice were handled according to the guidelines for the humane care and use of experimental animals, and the procedures used were approved by the Stony Brook University Institutional Animal Care and Use Committee.

Bone marrow isolation and culture conditions. Bone marrow was isolated from femur exudates of 6- to 8-week-old female C57BL/6 wild-type (Jackson Laboratories), *Caspase-1$^{-/-}$* (34), *Caspase-11$^{-/-}$* (35), or *Caspase-1/11$^{-/-}$* (36) mice or 129 wild-type or *Iqgap1$^{-/-}$* (37) mice as previously described (38). At 18 h prior to infection, BMDMs were seeded into tissue culture plates in Dulbecco's modified Eagle medium (Invitrogen) supplemented with 10% fetal bovine serum (HyClone), 15% L-cell-conditioned medium, 1 mM sodium pyruvate, 2 mM glutamate, and 100 ng/ml *E. coli* LPS (Sigma). BMDMs were used to seed six-well plates at

a density of 0.8×10^6 cells/well for all of the experiments except those in Fig. 3, where 48-well plates were seeded at 2.0×10^5 cells/well.

Macrophage infection or stimulation conditions. LPS-primed BMDMs were left uninfected or infected with *Y. pseudotuberculosis* grown under the conditions described above at a multiplicity of infection (MOI) of 30. Tissue culture plates were centrifuged for 5 min at 95 $\times g$ to facilitate the contact of yersiniae with BMDMs. Plates containing BMDMs were subsequently incubated at 37°C with 5% CO$_2$. At 90 min postinfection, cell supernatants were collected and analyzed for secreted IL-1β and LDH release while cell lysates were harvested for Western blotting of host proteins. As a positive control for activation of caspase-1, BMDMs were primed with 100 ng/ml *E. coli* LPS for 4 h and subsequently given 2.5 mM adenosine triphosphate (ATP) for 1 h.

Western blotting of macrophage cell lysates. BMDMs were washed twice with cold Hanks balanced salt solution to remove residual phenol red and lysed in lysis buffer (1% NP-40, 150 mM NaCl, 50 mM Tris-HCl [pH 8.0], protease inhibitor cocktail [Complete, Mini, EDTA-free; Roche]). Proteins were resolved by SDS-PAGE with NuPAGE Novex 4 to 12% Bis-Tris gels (Invitrogen) unless indicated otherwise, transferred onto a polyvinylidene difluoride (PVDF) membrane, and probed with rabbit polyclonal anti-caspase-1 (Santa Cruz Biotechnologies), rabbit

polyclonal anti-RSK1 (Abcam), and mouse monoclonal anti-IQGAP1 (BD Biosciences) antibodies. Horseradish peroxidase (HRP)-conjugated anti-rabbit (Cell Signaling) and anti-mouse (Jackson ImmunoResearch) antibodies were used as secondary reagents. To control for loading, Western blots were stripped and reprobed with anti-β-actin antibody conjugated to HRP (Sigma-Aldrich). Signals in Western blot assays were detected with Amersham ECL Prime Western blotting detection reagent (GE Healthcare).

ELISA. Levels of secreted IL-1β in supernatants collected from BMDMs were analyzed with a commercially available ELISA kit (R&D Biosystems) according to the manufacturer's instructions.

Cytotoxicity assay. The LDH released into supernatants of BMDMs was quantified with the LDH Cytotoxicity Assay kit (Clontech) according to the manufacturer's instructions.

Analysis of Yop secretion. Following growth of *Yersinia* cultures as described above, bacteria were removed by centrifugation and trichloroacetic acid (10%, wt/vol) was added to the supernatants to precipitate and collect secreted Yops as previously described (22). Samples were subsequently processed for Western blotting with mouse monoclonal antibodies (6-1CE or 2A3.3A8.1A2) that recognize epitopes in the N-terminal region of YopM (a gift from Susan Straley, University of Kentucky), mouse monoclonal anti-YopB antibodies (76.15, 190.11, or 328.1 [unpublished data]), or mouse monoclonal anti-YopE antibodies (149.27 or 202.19 [unpublished data]).

Purification of GST-YopM proteins. *E. coli* strains harboring pGEX-2T, pGEX-2T YopM^{KIM}, pGEX-2T YopM^{32777}, pDEST15 YopM$^{KIM\Delta6\text{-}15}$, or pDEST15 YopM$^{KIM\Delta12\text{-}C}$ (22) were grown in LB at 37°C to an optical density (OD) at 600 nm of 0.3 to 0.6. Isopropyl-β-D-thiogalactopyranoside (IPTG) was then added to a final concentration of 0.1 mM, and the cultures were grown for an additional 4 h. Bacteria were collected by centrifugation and lysed with Lysonase and Bugbuster reagents (Novagen) according to the manufacturer's instructions. Supernatants containing bacterial proteins were added to GST-Bind Resin (Novagen) and incubated for 30 min at 4°C on a rotating shaker. Samples were washed, and bound GST and GST-fused proteins were eluted according to the manufacturer's instructions. Purified proteins were dialyzed against PBS and used for GST pulldown assays or stored at −80°C.

GST pulldown assay. Ten micrograms of purified GST or GST-fused protein was added to 20 μl of GST-Bind Resin (Novagen) and incubated at 4°C for 30 min. Beads were then washed three times with 1× GST Bind/Wash Buffer (Novagen). Uninfected, LPS-primed or LPS- and ATP-treated BMDMs were incubated in lysis buffer as described above, and the resulting lysates were added to the beads and incubated for 2 h at 4°C on a rotating shaker. Resin-containing bound proteins were washed four times in lysis buffer and boiled in sample buffer, and the eluted proteins were separated by SDS-PAGE. Proteins were transferred to PVDF membranes, and Western blotting was performed as described above.

Silver staining and mass spectrometry. Samples from GST pulldown assays were resolved by SDS-PAGE. Gels were subsequently stained with the SilverQuest Stain kit (Invitrogen) according to the manufacturer's instructions. Specific bands were excised from the gel, fragmented by trypsin digestion, and subjected to analysis by liquid chromatography-tandem mass spectrometry (LC-MS/MS).

Yop translocation assays. Yop translocation assays were performed as previously described (39). Briefly, infected BMDMs were incubated in lysis buffer as described above and the soluble fraction of the lysate was collected and analyzed for the presence of YopM by Western blotting as described above.

Fluorescence microscopy. BMDMs were seeded onto glass coverslips pretreated with ethanol and acetone and sterilized to remove contaminants. BMDMs were left uninfected or infected as described above, except that the tissue culture medium was supplemented with 0.5 mM IPTG to induce GFP expression. BMDMs were washed twice with PBS, fixed with 2.5% paraformaldehyde, permeabilized with 0.1% Triton X-100, and blocked with bovine serum albumin as previously described (40).

BMDMs were incubated with a primary rabbit anti-NLRP3 polyclonal antibody (Santa Cruz Biotechnologies). Binding of the primary antibody was visualized by the addition of Alexa Fluor 594-conjugated anti-rabbit antibody (Invitrogen), and DNA was stained by the addition of 4,6′-diamidino-2-phenylindole (DAPI) dilactate. Coverslips were mounted onto glass slides with ProLong Gold antifade reagent (Invitrogen) and imaged with an Axiovert S100 (Zeiss) with a 32× objective. Images were taken with a SPOT camera (Diagnostic Instruments) and processed with Adobe Photoshop CS 5.1.

Statistical analysis. Experimental data analyzed for significance with GraphPad Prism 6.0 were from at least three independent experiments. Probability (P) values for IL-1β and LDH experiments were calculated by one-way analysis of variance (ANOVA) or grouped two-way ANOVA with Turkey's multiple-comparison posttest. P values from mouse survival experiments were calculated by log rank test. P values of <0.05 were considered significant.

SUPPLEMENTAL MATERIAL

Supplemental material for this article may be found at http://mbio.asm.org/lookup/suppl/doi:10.1128/mBio.01402-14/-/DCSupplemental.

Figure S1, DOCX file, 0.1 MB.
Figure S2, TIF file, 1.2 MB.
Figure S3, TIF file, 2.4 MB.

REFERENCES

1. **Medzhitov R.** 2007. Recognition of microorganisms and activation of the immune response. Nature **449:**819–826. http://dx.doi.org/10.1038/nature06246.
2. **Janeway CA, Jr, Medzhitov R.** 2002. Innate immune recognition. Annu. Rev. Immunol. **20:**197–216. http://dx.doi.org/10.1146/annurev.immunol.20.083001.084359.
3. **Akira S, Takeda K, Kaisho T.** 2001. Toll-like receptors: critical proteins linking innate and adaptive immunity. Nat. Immunol. **2:**675–680. http://dx.doi.org/10.1038/90609.
4. **Schroder K, Tschopp J.** 2010. The inflammasomes. Cell **140:**821–832. http://dx.doi.org/10.1016/j.cell.2010.01.040.
5. **Mariathasan S, Weiss DS, Newton K, McBride J, O'Rourke K, Roose-Girma M, Lee WP, Weinrauch Y, Monack DM, Dixit VM.** 2006. Cryopyrin activates the inflammasome in response to toxins and ATP. Nature **440:**228–232. http://dx.doi.org/10.1038/nature04515.
6. **Bauernfeind FG, Horvath G, Stutz A, Alnemri ES, MacDonald K, Speert D, Fernandes-Alnemri T, Wu J, Monks BG, Fitzgerald KA, Hornung V, Latz E.** 2009. Cutting edge: NF-kappaB activating pattern recognition and cytokine receptors license NLRP3 inflammasome activation by regulating NLRP3 expression. J. Immunol. **183:**787–791. http://dx.doi.org/10.4049/jimmunol.0901363.
7. **Miao EA, Warren SE.** 2010. Innate immune detection of bacterial virulence factors via the NLRC4 inflammasome. J. Clin. Immunol. **30:**502–506. http://dx.doi.org/10.1007/s10875-010-9386-5.
8. **Cunha LD, Zamboni DS.** 2013. Subversion of inflammasome activation and pyroptosis by pathogenic bacteria. Front. Cell. Infect. Microbiol. **3:**76. http://dx.doi.org/10.3389/fcimb.2013.00076.
9. **Bergsbaken T, Fink SL, Cookson BT.** 2009. Pyroptosis: host cell death and inflammation. Nat. Rev. Microbiol. **7:**99–109. http://dx.doi.org/10.1038/nrmicro2070.
10. **Cornelis GR.** 2006. The type III secretion injectisome. Nat. Rev. Microbiol. **4:**811–825. http://dx.doi.org/10.1038/nrmicro1526.
11. **Viboud GI, Bliska JB.** 2005. Yersinia outer proteins: role in modulation of

host cell signaling responses and pathogenesis. Annu. Rev. Microbiol. **59:** 69–89. http://dx.doi.org/10.1146/annurev.micro.59.030804.121320.

12. **Shin H, Cornelis GR.** 2007. Type III secretion translocation pores of *Yersinia enterocolitica* trigger maturation and release of proinflammatory IL-1beta. Cell. Microbiol. **9:**2893–2902. http://dx.doi.org/10.1111/j.1462-5822.2007.01004.x.

13. **Bergsbaken T, Cookson BT.** 2007. Macrophage activation redirects *Yersinia*-infected host cell death from apoptosis to caspase-1-dependent pyroptosis. PLoS Pathog. **3**(11):e161. http://dx.doi.org/10.1371/journal.ppat.0030161.

14. **Brodsky IE, Palm NW, Sadanand S, Ryndak MB, Sutterwala FS, Flavell RA, Bliska JB, Medzhitov R.** 2010. A *Yersinia* effector protein promotes virulence by preventing inflammasome recognition of the type III secretion system. Cell Host Microbe **7:**376–387. http://dx.doi.org/10.1016/j.chom.2010.04.009.

15. **Nemeth J, Straley SC.** 1997. Effect of *Yersinia pestis* YopM on experimental plague. Infect. Immun. **65:**924–930.

16. **Leung KY, Reisner BS, Straley SC.** 1990. YopM inhibits platelet aggregation and is necessary for virulence of *Yersinia pestis* in mice. Infect. Immun. **58:**3262–3271.

17. **LaRock CN, Cookson BT.** 2012. The *Yersinia* virulence effector YopM binds caspase-1 to arrest inflammasome assembly and processing. Cell Host Microbe **12:**799–805. http://dx.doi.org/10.1016/j.chom.2012.10.020.

18. **Evdokimov AG, Anderson DE, Routzahn KM, Waugh DS.** 2001. Unusual molecular architecture of the *Yersinia pestis* cytotoxin YopM: a leucine-rich repeat protein with the shortest repeating unit. J. Mol. Biol. **312:**807–821. http://dx.doi.org/10.1006/jmbi.2001.4973.

19. **McDonald C, Vacratsis PO, Bliska JB, Dixon JE.** 2003. The *Yersinia* virulence factor YopM forms a novel protein complex with two cellular kinases. J. Biol. Chem. **278:**18514–18523. http://dx.doi.org/10.1074/jbc.M301226200.

20. **Hentschke M, Berneking L, Belmar Campos C, Buck F, Ruckdeschel K, Aepfelbacher M.** 2010. *Yersinia* virulence factor YopM induces sustained RSK activation by interfering with dephosphorylation. PLoS One **5**(10): e13165. http://dx.doi.org/10.1371/journal.pone.0013165.

21. **McCoy MW, Marré ML, Lesser CF, Mecsas J.** 2010. The C-terminal tail of *Yersinia pseudotuberculosis* YopM is critical for interacting with RSK1 and for virulence. Infect. Immun. **78:**2584–2598. http://dx.doi.org/10.1128/IAI.00141-10.

22. **McPhee JB, Mena P, Bliska JB.** 2010. Delineation of regions of the *Yersinia* YopM protein required for interaction with the RSK1 and PRK2 host kinases and their requirement for interleukin-10 production and virulence. Infect. Immun. **78:**3529–3539. http://dx.doi.org/10.1128/IAI.00269-10.

23. **Boland A, Havaux S, Cornelis GR.** 1998. Heterogeneity of the *Yersinia* YopM protein. Microb. Pathog. **25:**343–348. http://dx.doi.org/10.1006/mpat.1998.0247.

24. **Weissbach L, Settleman J, Kalady MF, Snijders AJ, Murthy AE, Yan YX, Bernards A.** 1994. Identification of a human rasGAP-related protein containing calmodulin-binding motifs. J. Biol. Chem. **269:**20517–20521.

25. **Kayagaki N, Warming S, Lamkanfi M, Vande Walle L, Louie S, Dong J, Newton K, Qu Y, Liu J, Heldens S, Zhang J, Lee WP, Roose-Girma M, Dixit VM.** 2011. Non-canonical inflammasome activation targets caspase-11. Nature **479:**117–121. http://dx.doi.org/10.1038/nature10558.

26. **Rathinam VA, Vanaja SK, Waggoner L, Sokolovska A, Becker C, Stuart LM, Leong JM, Fitzgerald KA.** 2012. TRIF licenses caspase-11-dependent NLRP3 inflammasome activation by gram-negative bacteria. Cell **150:** 606–619. http://dx.doi.org/10.1016/j.cell.2012.07.007.

27. **Buss C, Müller D, Rüter C, Heusipp G, Schmidt MA.** 2009. Identification and characterization of Ibe, a novel type III effector protein of A/E pathogens targeting human IQGAP1. Cell. Microbiol. **11:**661–677. http://dx.doi.org/10.1111/j.1462-5822.2009.01284.x.

28. **McLaughlin LM, Govoni GR, Gerke C, Gopinath S, Peng K, Laidlaw G, Chien YH, Jeong HW, Li Z, Brown MD, Sacks DB, Monack D.** 2009. The *Salmonella* SPI2 effector SseI mediates long-term systemic infection by modulating host cell migration. PLoS Pathog. **5**(11):e1000671. http://dx.doi.org/10.1371/journal.ppat.1000671.

29. **Kim H, White CD, Sacks DB.** 2011. IQGAP1 in microbial pathogenesis: targeting the actin cytoskeleton. FEBS Lett. **585:**723–729. http://dx.doi.org/10.1016/j.febslet.2011.01.041.

30. **White CD, Erdemir HH, Sacks DB.** 2012. IQGAP1 and its binding proteins control diverse biological functions. Cell. Signal. **24:**826–834. http://dx.doi.org/10.1016/j.cellsig.2011.12.005.

31. **Palmer LE, Hobbie S, Galán JE, Bliska JB.** 1998. YopJ of *Yersinia pseudotuberculosis* is required for the inhibition of macrophage TNF-alpha production and downregulation of the MAP kinases p38 and JNK. Mol. Microbiol. **27:**953–965. http://dx.doi.org/10.1046/j.1365-2958.1998.00740.x.

32. **Zhang Y, Murtha J, Roberts MA, Siegel RM, Bliska JB.** 2008. Type III secretion decreases bacterial and host survival following phagocytosis of *Yersinia pseudotuberculosis* by macrophages. Infect. Immun. **76:** 4299–4310. http://dx.doi.org/10.1128/IAI.00183-08.

33. **Li P, Allen H, Banerjee S, Franklin S, Herzog L, Johnston C, McDowell J, Paskind M, Rodman L, Salfeld J, Towne E, Tracey D, Wardell S, Wei F-Y, Wong W, Kamen R, Seshadri T.** 1995. Mice deficient in IL-1 beta-converting enzyme are defective in production of mature IL-1 beta and resistant to endotoxic shock. Cell **80:**401–411. http://dx.doi.org/10.1016/0092-8674(95)90490-5.

34. **Case CL, Kohler LJ, Lima JB, Strowig T, de Zoete MR, Flavell RA, Zamboni DS, Roy CR.** 2013. Caspase-11 stimulates rapid flagellin-independent pyroptosis in response to Legionella pneumophila. Proc. Natl. Acad. Sci. U. S. A. **110:**1851–1856. http://dx.doi.org/10.1073/pnas.1211521110.

35. **Wang S, Miura M, Jung YK, Zhu H, Li E, Yuan J.** 1998. Murine caspase-11, an ICE-interacting protease, is essential for the activation of ICE. Cell **92:**501–509. http://dx.doi.org/10.1016/S0092-8674(00)80943-5.

36. **Kuida K, Lippke JA, Ku G, Harding MW, Livingston DJ, Su MS, Flavell RA.** 1995. Altered cytokine export and apoptosis in mice deficient in interleukin-1 beta converting enzyme. Science **267:**2000–2003. http://dx.doi.org/10.1126/science.7535475.

37. **Li S, Wang Q, Chakladar A, Bronson RT, Bernards A.** 2000. Gastric hyperplasia in mice lacking the putative Cdc42 effector IQGAP1. Mol. Cell. Biol. **20:**697–701. http://dx.doi.org/10.1128/MCB.20.2.697-701.2000.

38. **Celada A, Gray PW, Rinderknecht E, Schreiber RD.** 1984. Evidence for a gamma-interferon receptor that regulates macrophage tumoricidal activity. J. Exp. Med. **160:**55–74. http://dx.doi.org/10.1084/jem.160.1.55.

39. **Ryndak MB, Chung H, London E, Bliska JB.** 2005. Role of predicted transmembrane domains for type III translocation, pore formation, and signaling by the *Yersinia pseudotuberculosis* YopB protein. Infect. Immun. **73:**2433–2443. http://dx.doi.org/10.1128/IAI.73.4.2433-2443.2005.

40. **Pujol C, Bliska JB.** 2003. The ability to replicate in macrophages is conserved between *Yersinia pestis* and *Yersinia pseudotuberculosis*. Infect. Immun. **71:**5892–5899. http://dx.doi.org/10.1128/IAI.71.10.5892-5899.2003.

41. **Simonet M, Falkow S.** 1992. Invasin expression in *Yersinia pseudotuberculosis*. Infect. Immun. **60:**4414–4417.